

## Displacement Distribution Measured by Directional Acoustic Field Generated by Dual Ultrasound Excitation to Estimate Viscoelasticity of Muscle Tissues

筋組織の粘弾性推定を目指した双方向超音波加振による指向性音場の変位分布の計測

Hibiki Kawamura<sup>1,†</sup>, Shohei Mori<sup>1</sup>, Mototaka Arakawa<sup>2,1</sup> and Hiroshi Kanai<sup>1,2</sup>

(<sup>1</sup> Grad. School of Eng., Tohoku Univ.; <sup>2</sup> Grad. School of Biomed. Eng., Tohoku Univ.)

川村 響<sup>1,†</sup>, 森 翔平<sup>1</sup>, 荒川 元孝<sup>2,1</sup>, 金井 浩<sup>1,2</sup> (東北大院 工,<sup>2</sup>東北大院 医工)

### 1. Introduction

The elasticity of muscle tissues is closely related to the progression of lesions. The muscle tissue has anisotropy because it is composed of bundles of muscle fibers. Therefore, it is necessary to consider the anisotropy for the evaluation.

We have proposed a method to estimate the viscoelasticity of the biological tissues by measuring frequency characteristics of displacement and stress generated by dual ultrasound excitation.<sup>1)</sup> The acoustic field generated by dual ultrasound excitation could have directivity. It is necessary to understand this directivity for the evaluation of anisotropic tissues such as muscle.

In the present study, we measured the directivity of the acoustic field generated by ultrasound excitation. Furthermore, we measured the displacement distribution on a phantom surface generated by ultrasound excitation.

### 2. Materials and Method

**Fig. 1** shows the experimental arrangement in the present study. Two point-focus transducers (TR1, TR2) with a center frequency  $f_0$  of 1 MHz, an aperture half-angle of  $22.6^\circ$ , an effective aperture width of 50 mm, and a focal length of 60 mm were used for ultrasound excitation. They were opposed with an irradiation angle of  $35^\circ$  to the phantom. The focal points of two transducers coincided at the center on the phantom surface.

Sinusoidal signals with frequencies of  $f_0$  and  $(f_0 + \Delta f)$  generated by a function generator (Tektronix, Inc., AFG2020) were summed up, and applied to the transducers. Then, the acoustic radiation pressure on the phantom surface locally pinches along the  $x$ -axis, which causes shear strain in the  $z$ -axis direction at  $\Delta f$ .<sup>2)</sup> The excitation frequency  $\Delta f$  was set as 20 Hz.

For measurement of the acoustic field, we replaced the phantom in Fig. 1 with a hydrophone (Toray Industries, Inc., NH8133). It was installed parallel to the  $z$ -axis to measure the  $z$ -axis component of the sound pressure. The output signal of the hydrophone was input to the FFT analyzer (Ono Sokki Co. Ltd., CF-930), and the frequency spectrum was acquired to extract the excitation frequency  $\Delta f$  component of the sound pressure.

The phantom simulating biological soft

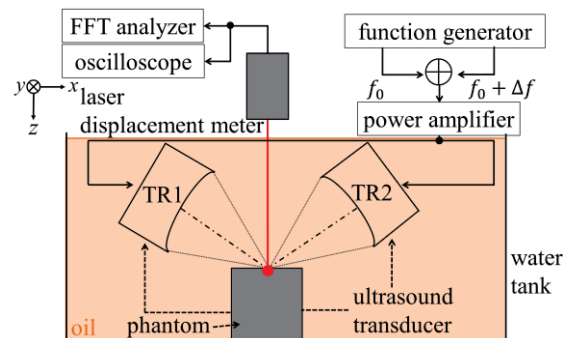


Fig. 1. Experimental arrangement employed in the present study.

tissues with a size of  $40 \times 40 \times 43 \text{ mm}^3$  was prepared by Asker-C hardness 7 urethane resin with a 2-wt% graphite. The displacement on the phantom surface in the  $z$ -axis direction was measured with the laser displacement meter (Keyence Corp., LK-G80). The output signal was input to the FFT analyzer to extract the  $\Delta f$  component of the displacement. The measurement region was  $10 \times 10 \text{ mm}^2$  on the  $x$ - $y$  plane centered on the focal point of the two transducers.

### 3. Results

#### 3.1 Acoustic field

**Figs. 2(a) and 2(b)** show the acoustic field by the dual excitation and the single excitation using the only TR1, respectively. They were normalized by each maximum sound pressure. In Fig. 2(a), the sound pressure in the  $y$ -axis direction extends about twice as much as that in the  $x$ -axis direction from the -10-dB contour line. In addition, it spread in the shape of the figure “eight” in the  $y$ -axis direction from the -20-dB contour line. In Fig. 2(b), the sound pressure at the focal point was high. Moreover, the sound pressure spread in the shape of the figure “eight” in the  $x$ -axis direction from the -35-dB contour line. Thus, there was directivity of the acoustic field in the  $x$ -axis direction by the single excitation and in the  $y$ -axis direction by the dual excitation. The maximum amplitude difference of the sound pressure was about 30-dB in both Figs. 2(a) and 2(b).

#### 3.2 Displacement distribution on phantom

**Figs. 3(a) and 3(b)** show the displacement distribution by the dual excitation and the single excitation using the only TR1, respectively. In Fig.

3(a), displacements in the  $y$ -axis direction spread about twice compared to those in the  $x$ -axis direction from contour lines. Moreover, the shape of the figure eight was also observed. In Fig. 3(b), the displacements spread almost uniformly in both  $x$ - and  $y$ -axes directions from the contour lines. Thus, the displacement distribution was less affected by the directivity of the acoustic field. The maximum difference of the displacement was about 13 dB in both Figs. 3(a) and 3(b).

#### 4. Discussion

The acoustic radiation pressure depends on the energy density difference.<sup>3)</sup> Therefore, the acoustic radiation pressure is proportional to the square of the sound pressure. According to Hooke's law, excitation stress is linearly related to the displacement. Thus, the displacement is proportional to the square of the sound pressure. Therefore, this is the factor that the maximum differences of displacements in Fig. 3 became smaller than those of sound pressures in Fig. 2.

If the strong sound pressure is applied locally, the displacement occurs not only the applied point but also around it because the object is elastically continuous. Therefore, the measured displacement distribution becomes the sum of the displacement

generated by the strong sound pressure in the directional acoustic field and that generated indirectly by the large sound pressure near the focal point. Therefore, the directionality of the displacement distribution in Fig. 3 became less than that of the acoustic field in Fig. 2.

#### 5. Conclusion

We measured the directivity of the acoustic field generated by ultrasound excitation and the displacement distribution of the phantom generated by the directional acoustic field. The directivities of the generated acoustic field were greatly different between single and dual ultrasound excitations. Furthermore, we measured the displacement distribution reflecting the directivity in dual excitation. In future, we will apply this method to objects with anisotropy and discuss the possibility of anisotropy detection.

#### References

1. R. Watanabe, M. Arakawa, and H. Kanai: Jpn. J. Appl. Phys. **57** (2018) 07LF09.
2. J. Yamaguchi, H. Hasegawa, and H. Kanai: J. Med. Ultrasounds. **39** (2012) 279.
3. G. R. Torr: Am. J. Phys. **52** (1984) 402.

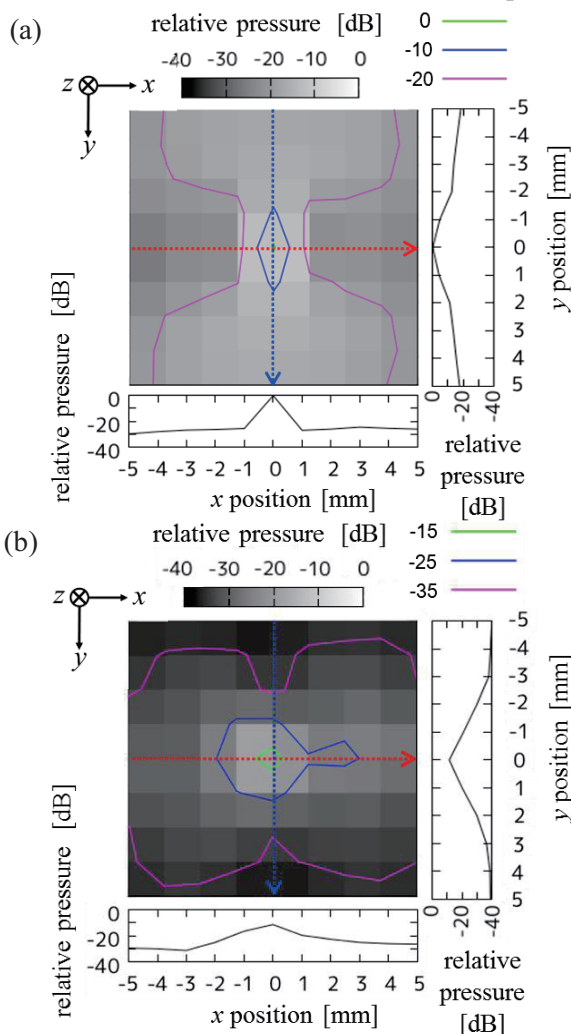


Fig. 2. Acoustic field generated by (a) dual excitation and (b) single excitation.

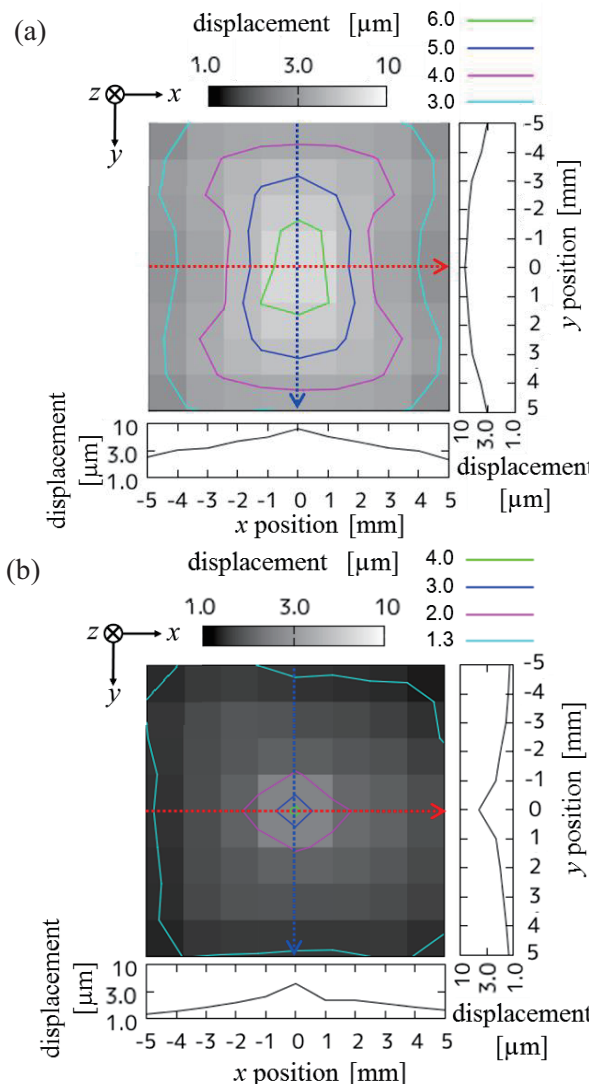


Fig. 3. Displacement distribution on the phantom generated by (a) dual excitation and (b) single excitation.